Journal of Marine Research, 64, 393–406, 2006

Inferring mixed-layer depth variability from Argo observations in the western Indian Ocean

by T. V. S. Udaya Bhaskar[1,2], D. Swain[1] and M. Ravichandran[1]

ABSTRACT

The seasonal and spatial variability of mixed layer depth (MLD) was examined in the Western Indian Ocean (WIO) (30E – 80E and 10S – 30N) for three consecutive years starting from June 2002 – May 2005 using Argo temperature and salinity (T/S) profiles. These were compared with MLD estimates from World Ocean Atlas 2001 (WOA01) T/S data. Temporal and spatial variability of MLD estimated from Argo T/S profiles were found to correspond well with the MLD obtained from WOA01 T/S data. However, slight deviations in the form of months of occurrence of minima and maxima MLDs were observed. MLD from WOA01 climatology is underestimated compared to MLD from Argo for almost the entire three years of study. It is also observed that MLD variability features as brought out by both the data sets followed the dynamics that govern the mixed layer variability in this region.

1. Introduction

The ocean's effect on weather and climate is governed largely by processes occurring in the few tens of meters of water bordering the ocean surface. The upper ocean is the most variable, accessible and dynamically most active part of the marine environment. It connects the deeper ocean, where the heat and fresh water are stored and released on longer time scales, with surface forcing from winds, heat and fresh water. Exposed to these actions, the oceanic surface layer is a region of vigorous mixing. This process produces a layer of uniform properties called the mixed layer and the depth of this layer is referred to as the mixed layer depth (MLD). MLD is one of the important parameters in physical oceanography which plays a vital role in air-sea heat exchange. The transfer of mass, momentum and energy across the mixed layer provides the source of all oceanic motions. The thickness of this layer determines the heat content and mechanical inertia that directly interact with the atmosphere.

Temporal variabilities of MLD are in a way directly linked to processes occurring in the mixed layer (Brainerd and Gregg, 1995). MLD varies on several temporal scales; viz., diurnal, intraseasonal, and seasonal (Fischer, 1997, 2000; Weller and Farmer, 1992; Babu *et al.*, 2004). In order to model the ocean's climate variability accurately, reliable information on the space-time variability of MLD is significant. In addition, the restriction of all biological activity

1. Indian National Center for Ocean Information Services, Hyderabad, India.
2. Corresponding author: ***email: uday@incois.gov.in***

to the upper layers of the ocean demands the need for accurate MLD estimates for biological studies (Morel and Andre, 1991; Longhurst, 1995). Until recently, MLD has been estimated using climatological temperature and salinity (T/S) profiles (e.g., Levitus, 1982; Suga and Hanawa, 1990; Montery and Levitus, 1997; Kara *et al.*, 2000) or, *in situ* temperature and/or density computed from *in situ* T/S observations obtained from CTDs (Lukas and Lindstrom, 1991; Ali and Sharma,1994; Thomson and Fine, 2003; de Boyer Montégut *et al.*, 2004). However, no single global definition for MLD has been agreed upon.

Owing to the limitation of *in situ* observations in terms of their spatial and temporal spreads and difficulty in defining MLD, several statistical and analytical models have attempted to estimate MLD (e.g., Price *et al.,* 1986; Chen *et al.*, 1994; Godfrey and Schiller, 1997; Schiller *et al.,* 1997). However, it is necessary to validate these model outputs with *in situ* observations to test their performance and finetune them.

To meet the demand for high quality hydrographic data on real/near-real time, the international Argo project was launched in 2000 under which several floats have been deployed worldwide. As of May 2005, 377 floats are active in the Indian Ocean region. These profiling floats have enormous application capabilities in terms of providing a real-time capability for measurement of T/S profiles within the upper 2000 m of the ocean. The data obtained from these floats can be used to describe the seasonal cycle and interannual variability of the upper ocean thermohaline circulation (Argo Science Team, 2001; Ravichandran *et al.*, 2004).

In the present analysis, we have estimated MLD based on the Argo float T/S profile data from June 2002 to May 2005 and studied its distribution and variability in the western Indian Ocean (WIO) [30E – 80E and 10S – 30N] during the same period. The profile density in the study region during the study period is shown in Figure 1. Since many of the oceanic studies carried out have relied on World Ocean Atlas 2001 (WOA01) (Conkright *et al.*, 2002), we have compared the MLD obtained from Argo float profiles (MLD_A) with those obtained using WOA01 climatology T/S profiles (MLD_W) to have a comparison between both the MLDs. We believe that the present study will be a useful contribution in understanding the regional and seasonal dependencies of MLD variability in WIO. Ohno *et al.* (2004) have used Argo data to estimate MLD and study its spatial and temporal distribution in the North Pacific. However, no such study has been carried out employing Argo float data for the North Indian Ocean, a region that is of high significance owing to its topography and contribution to regional and global climate variability.

2. Data and methodology

The data used in this study are the T/S profiles measured by the Argo floats in the WIO from June 2002 to May 2005. The profiles' data were obtained from the INCOIS web site (http://www.incois.gov.in/Incois/argo/argo_webGIS_intro.jsp#) which are made available by USGODAE and IFREMER. The climatological monthly mean T/S data of the WOA01 have been used for comparison.

Argo floats measure T/S from surface to 2000 m depth every 5/10 days. Out of 8337 available T/S profiles from June 2002 – May 2005 in the study area, 5962 profiles were selected

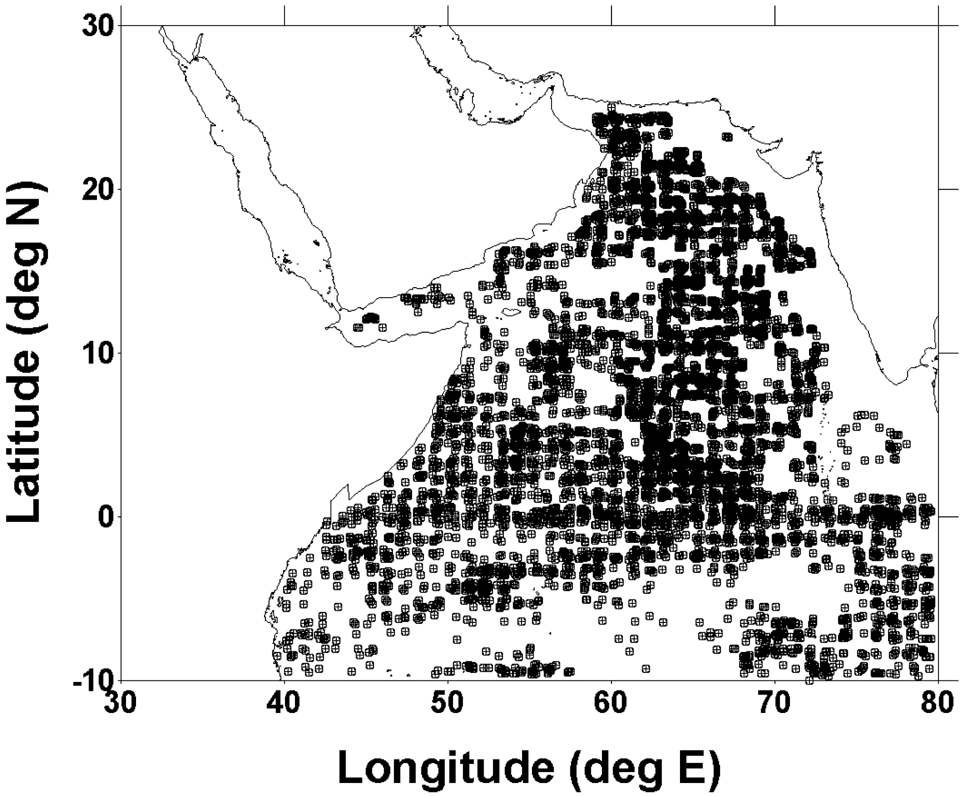

Figure 1. Map of Argo profile density in the study region for the period June 2002 – May 2005.

after applying the real time quality control checks like density inversion test, spike test and gradient test (see Wong *et al.*, 2004). Since data are unavailable at regular depths for all the floats, we interpolated the profiles linearly to 1 m depth resolution until 1000 m for all the observations.

For estimating MLD, density was first computed from the T/S measurements using the high-pressure equation of state (Millero *et al.*, 1980). MLD was then estimated as the depth at which the density is greater than the density at the surface by 0.125 kg m^{-3} (e.g., Levitus, 1982; Uehara *et al.* 2003; Suga *et al.* 2004; Ohno *et al.,* 2004). MLD_A computed from the T/S profiles was interpolated to regular grids of resolution 1° X 1° in the study region using the Kriging method. The error in the interpolation is presented as Kriging standard deviation (SD).

Kriging is based on the statistical principles and on the assumption that the parameter being interpolated can be treated as a regionalized variable which is true for MLD (de Boyer Montégut *et al.*, 2004). The advantage of Kriging as an objective analysis tool is that it is an exact interpolator, and the estimation error in the form of the Kriging SD (an analogy to the statistical SD) is provided. This method assumes that local means are not necessarily related to the population mean, and therefore uses only the sample in the local

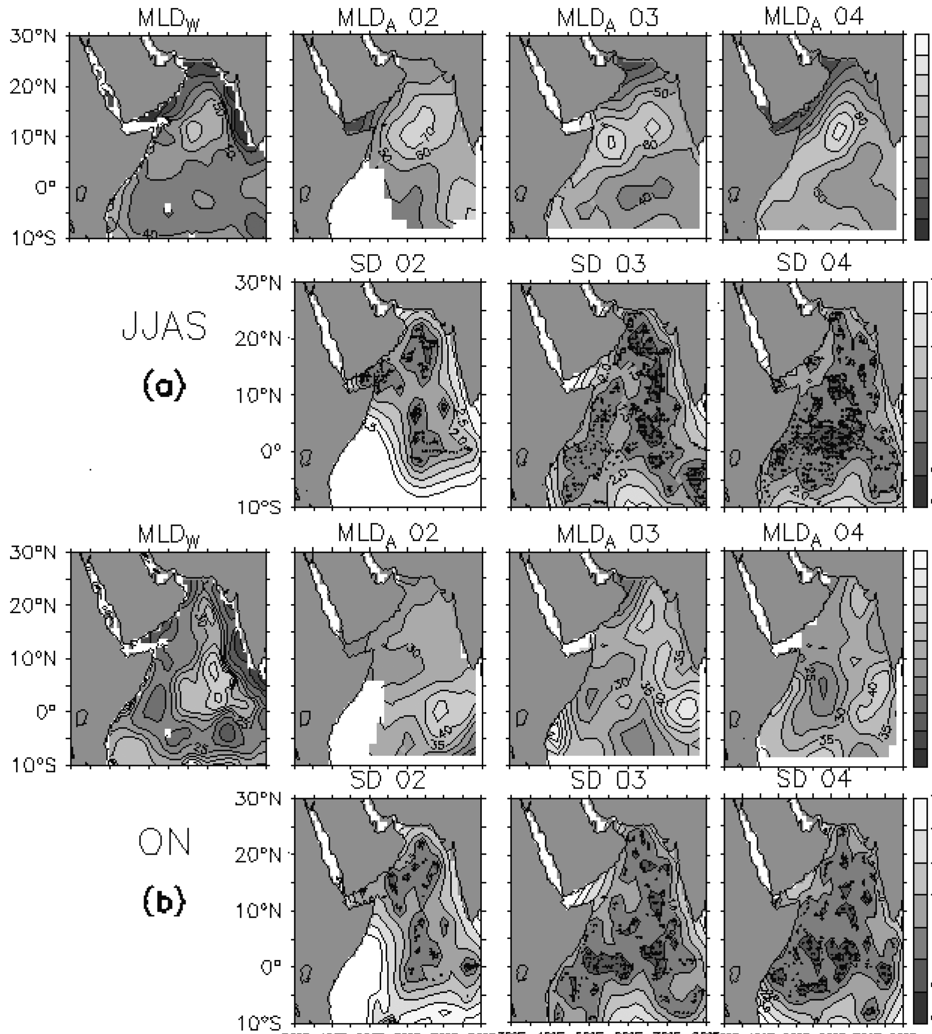

Figure 2. Seasonal means and Kriging Standard Deviation contours of MLD estimated from WOA01 (MLD_W) and Argo (MLD_A) for the seasons:(a) summer monsoon (JJAS), (b) post-monsoon (ON), (c) winter monsoon (DJF), and (d) pre-monsoon (MAM).

neighborhood of the estimation location. It builds a weighted average of those neighboring data so as to minimize the estimation variance which can be expressed in terms of the model covariances of the data (Wackernagel, 1998).

Our intention in this paper is to study MLD_A from limited data sets available from the initial phase of Argo floats deployment in the Indian Ocean region. Further, we compare these with MLD_W obtained with a similar definition in order to identify the difference between them. We also intend to observe the spatial and seasonal variability of MLD obtained from both the data

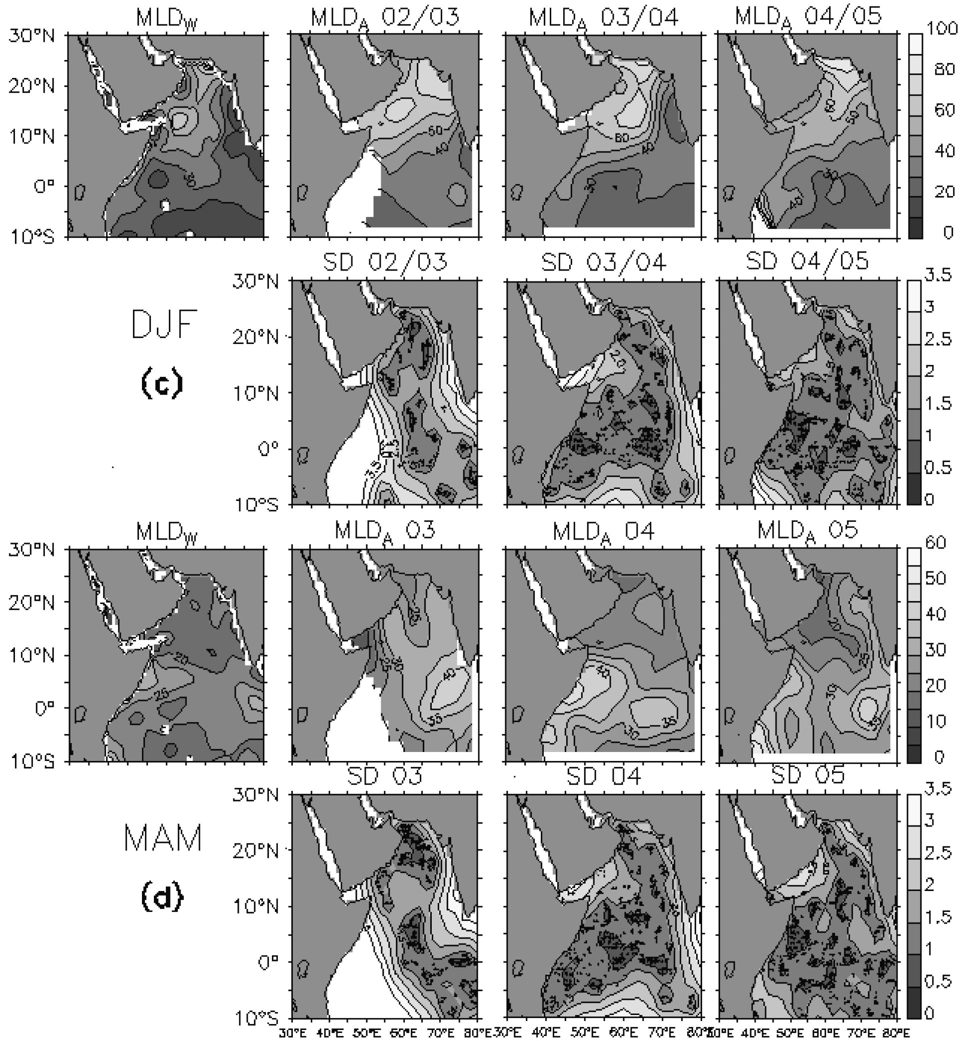

Figure 2. (Continued)

sets and we have also used outgoing longwave radiation (OLR) data from CDC (http://www.cdc.noaa.gov/) and QuikScat wind stress (WS) data obtained from IFREMER (ftp.ifremer.fr/ifremer/cersat/products/gridded/mwf-quikscat/data) during the study period to have a qualitative analysis of their influence on MLD variability.

3. Results and discussion

The spatial distribution of MLD_W and MLD_A are presented as seasonal means for the years 2002-2005 in Figure 2, for the months chosen to be representative of (a) Southwest

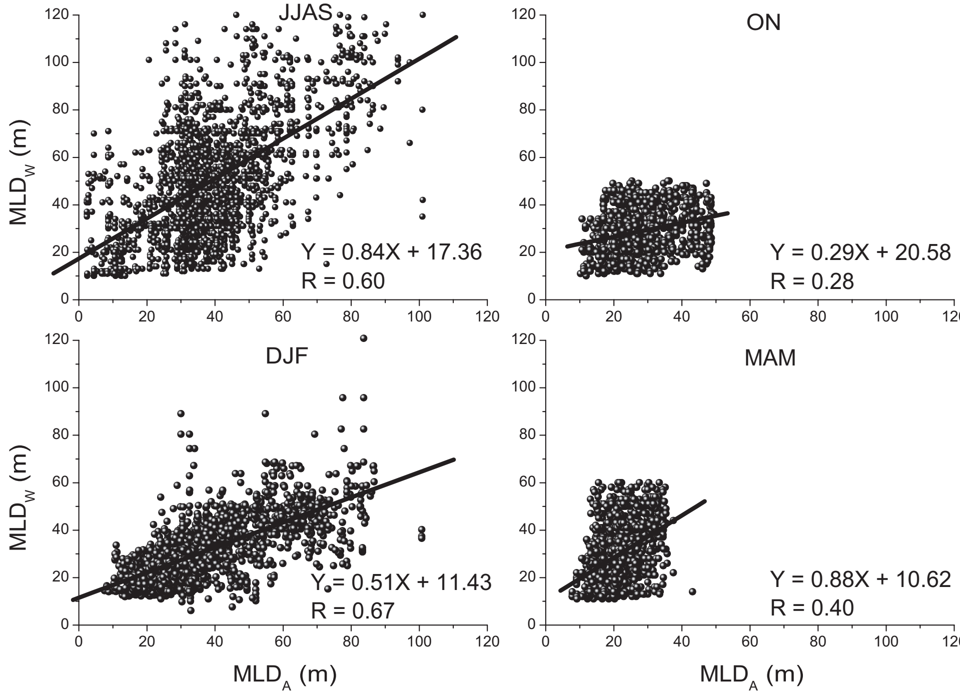

Figure 3. Seasonal Scatter of MLD estimated from WOA01 (MLD_W) and Argo (MLD_A) for the seasons summer monsoon (JJAS), post-monsoon (ON), winter monsoon (DJF), and pre- monsoon (MAM).

monsoon: June, July, August, September (JJAS), (b) Post-monsoon: October, November (ON), (c) Northeast monsoon: December, January, February (DJF), (d) Pre-monsoon: March, April, May (MAM). The SD contours that are representative of the errors in the objective analysis method (error plots for WOA01 are not provided as the available grided T/S data has been used directly for computation of MLD_W) have been presented in Figure 2. The SD plots further include the location of Argo profiles indicating the data densities. SD is large in regions with less number of profiles and is less in regions with large number of profiles. However, the maximum SD is confined to about 3.5 m for all the seasons.

Figure 3 depicts the scatter between MLD_A and MLD_W. The correlation coefficient (R) between MLD_A and MLD_W is 0.60, 0.28, 0.67 and 0.40 for southwest monsoon, post-monsoon, northeast monsoon, and pre-monsoon, respectively. The corresponding regression equations are also presented in Figure 3. Observations from Argo as well as WOA01 revealed that MLD is relatively shallow in the equatorial region through all the seasons of the year. However, a seasonal variation in MLD is observed in the North-Western Indian Ocean.

The North Indian Ocean is influenced by seasonally reversing monsoonal wind forcing, apart from winter cooling, radiative forcing and fresh-water forcing. All these factors affect

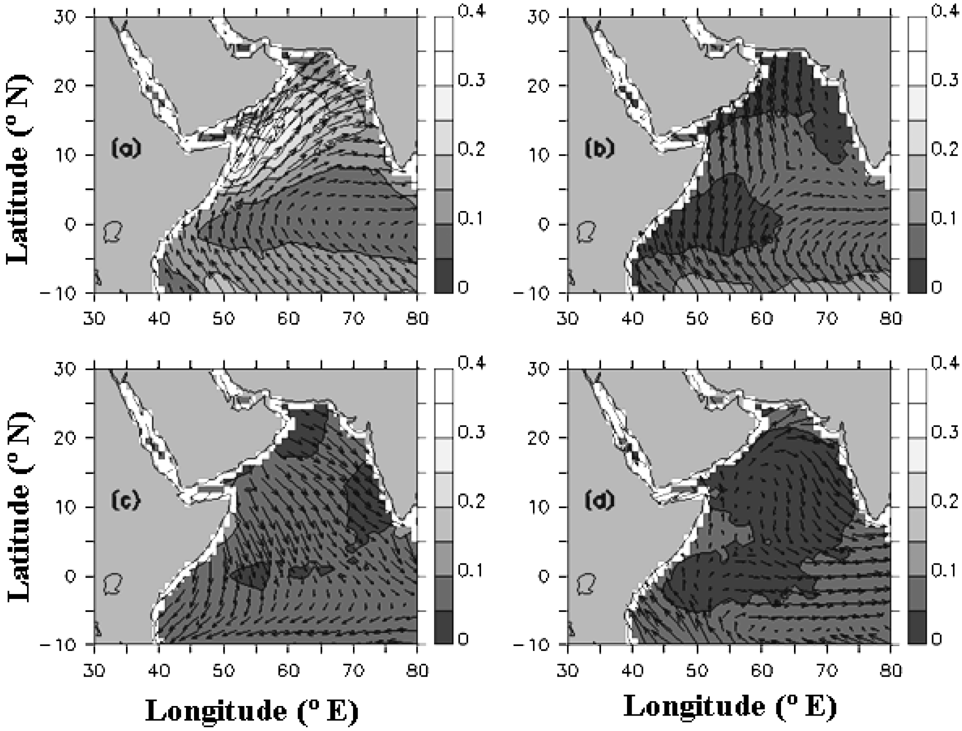

Figure 4. Seasonal averages of zonal and meridional wind stress vectors overlayed on seasonal average wind stress contours for the study period (a) Summer Monsoon (b) Post Monsoon (c) Winter Monsoon, (d) Pre Monsoon.

the mixed-layer dynamics and contribute to its variability. Prasad and Bahulayan (1996), Weller *et al.* (2002), and Prasad (2004) attribute variations in solar insolation, WS and buoyancy flux as the significant factors that determine the MLD variability in this region. The seasonal analysis presented below pertains to variations in MLD_A and MLD_W. Furthermore, we cross checked to see if the variability in MLD is in accordance with the dynamics that govern it. Qualitative analyses of seasonal averages of WS and OLR for the study period are presented in Figures 4 and 5 to support the observations.

a. Southhwest (SW) monsoon

During the SW monsoon season (JJAS), solar insolation decreases due to cloud cover and winds play a major role in determining the MLD, which changes in accordance with monsoon winds. This can be seen when comparing Figures 4a and 5a with Figure 2a. During this period, the MLD increases markedly in the interior Arabian Sea (AS) owing to Ekman convergence associated with strong, negative wind curl southeast of the Findlater jet axis (see Findlater, 1969) and shallows to its west (Duing and Leetma, 1980; McCreary and Kundu, 1989; Prasad and Bahulayan, 1996). In our analysis, this is seen by the

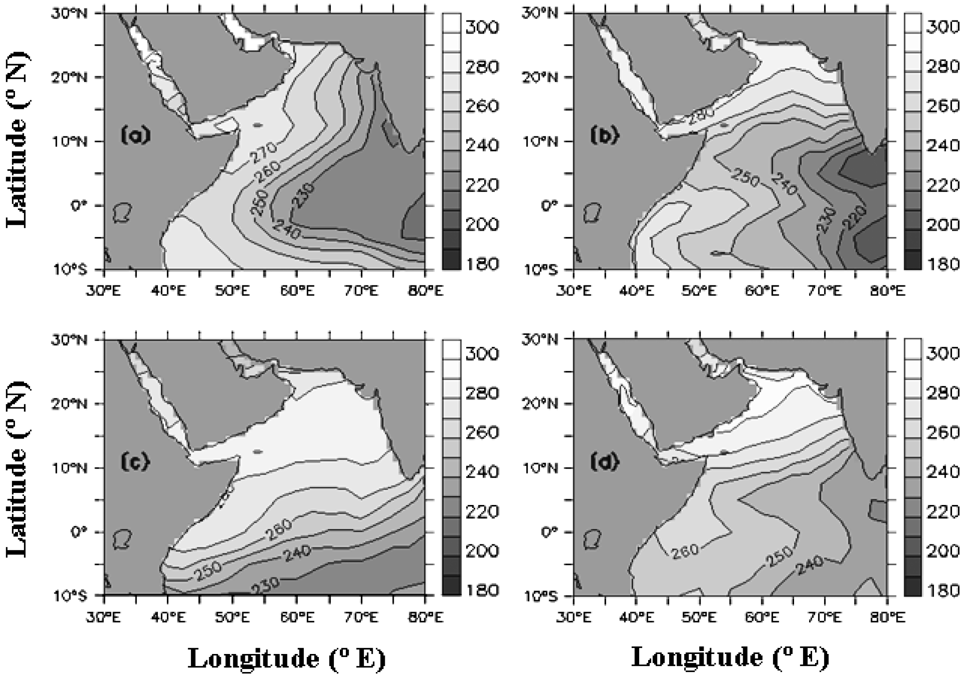

Figure 5. Contour plots of seasonal averages of outgoing longwave radiation (OLR).for the study period (a) Summer Monsoon, (b) Post Monsoon, (c) Winter Monsoon, and (d) Pre Monsoon.

deepening of MLD in the central AS (60E – 70E and 5N – 15N) and shallowing along the coast of Somalia, Arabia and northern most corners of the AS in case of both MLD_W, and MLD_A (Fig. 2a) in response to the prevailing SW monsoon winds (Fig. 4a). This contrasting phenomenon of deep and shallow MLD between the interior AS and western Arabian Coast persisted throughout the summer monsoon up to September and vanished with the onset of winter.

b. Post-monsoon

With the withdrawal of the southwest monsoon, the prevailing winds become westerlies, near and north of the equator along 60E to 90E. During this period (ON) there is a strong eastward current along the equator known as the Wyrtki jet (Wyrtki, 1973). A feature of high MLD surrounded by patches of low MLD for MLD_W starting from central AS and extending up to the equator is seen which is some what distinct compared to MLD_A for all the years of analysis. However, both the MLD estimates are shallow in the AS (north of 10N) and deeper from 10N to 10S. Along this region, MLD is observed to be deeper in the eastern part (around 80E) and shallower on the west (around 50E). From Figure 4b, we observe that winds have reduced and OLR has just started to pick up in the northern AS (Fig. 5b) during ON. The prevailing westerlies pile up water toward the east coast resulting in downward sloping of MLD from west to east (Ali and Sharma, 1994; O'Brien and Hurlburt, 1974). This phenomenon is clearly reflected in our analysis presented in Figure 2b. The month of November is characterized by northeasterly winds appearing in the AS, marking the beginning of northeast monsoon.

c. Northeast (NE) monsoon

During the NE monsoon (DJF), wind-stress forcing is weak (Fig. 4c), OLR is quite high (Fig. 5c), and convective mixing due to winter cooling plays a major role in determining MLD in the northern Indian Ocean. The local forcing by northeasterly winds helps to strengthen the Somali undercurrent flow in December and January, but negative wind-stress curl to its north weakens the current in February. MLD was observed to be deeper in AS with gradual decrease toward the equator and below. Prasad (2004) attribute the deepening of MLD in AS to negative surface heat flux and the associated temperature changes due to winter cooling during the NE monsoon. From our analysis (Fig. 2c), a band of low MLD is found to form between the equator and 10S. This low is observed consistently for the years 2002 – 2005 in the case of MLD_A. The gradual decrease of MLD toward the equator is due to change in solar insolation as one moves towards the southern hemisphere (Fig. 5c). A similar trend is also observed in the case of MLD_W.

d. Pre-monsoon

The pre-monsoon (MAM) is marked by a relative decrease in solar insolation as compared to DJF but significant reduction in wind activity. This is seen in Figure 5d with decrease in OLR values and less WS magnitude (Fig. 4d). Consequently, the northern Indian Ocean continues to warm up. A southward Somali undercurrent is present near the equator (5N – 0°) which develops during March in response to the forcing by wind in AS. By May, it is remotely forced by the radiation of Rossby waves from the west coast of India (eg: McCreary *et al.*, 1993). In our analysis, MLD (both MLD_A and MLD_W) was observed to have shallowed in the central AS during this period (Fig. 2d). However, the convergence of the southward- flowing Somali Current and northward-flowing East African Coastal Current deepens MLD along the coast of Africa in the vicinity of the equator (McCreary *et al.*, 1993; Prasad and Bahulayan, 1996) which is clearly observed in the present study.

e. MLD variability

We plotted MLD along the 64E longitude representing the central AS, to observe the latitudinal variability of MLD (Fig. 6) for each of the seasons spanning the analysis period. The figure reveals that MLD variability is quite high between 5N to 20N in the summer and winter monsoon seasons where as the variability is low in pre and post monsoons. From the latitudinal variability, we observe that the MLD difference between the two estimates is large when the MLD is deep. Kanegae and Kubota (2003) have carried out a similar analysis for the North Pacific Ocean and compared their results with Joint Environmental Data Analysis (JEDAC). They found that the MLD_A underestimates MLD from JEDAC

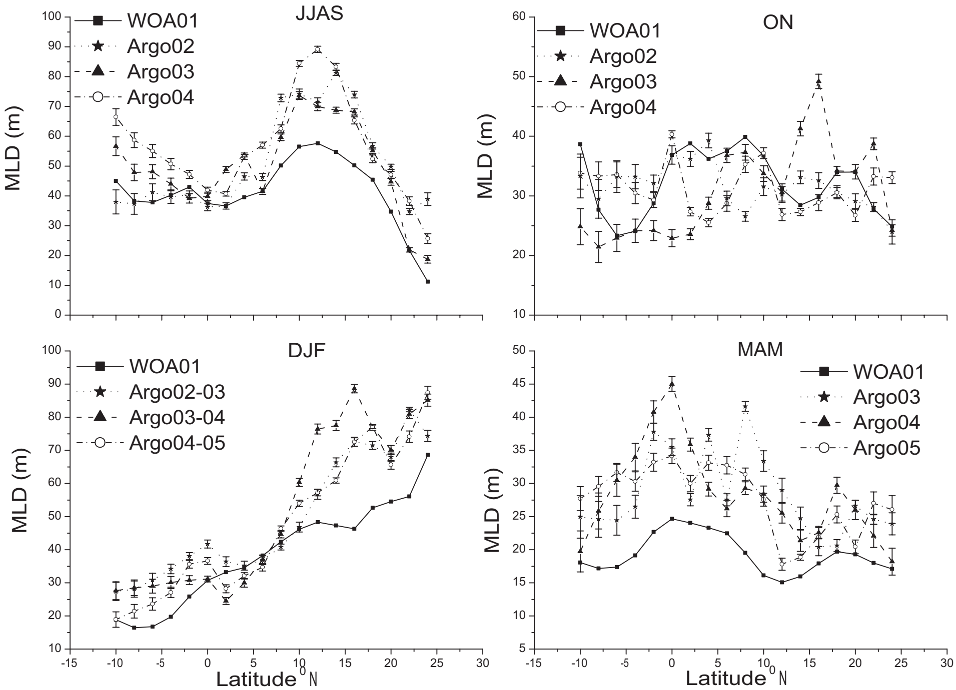

Figure 6. Latitudinal variability of MLD estimated from Argo along 64E longitude.

and the difference between both the estimates is high whenever MLD is deep in mid latitudes.

In order to observe the changes in MLD year to year, the central AS (60E – 70E and 5N – 15N) was chosen. There were 20 floats in this region with 1708 observations during the study period. A comparison of MLD_A for the seasons corresponding to years 2002, 2003, 2004, 2005 with MLD_W for this region is presented in Figure 7. Both MLD_A and MLD_W clearly show a semi-annual oscillation where one maxima is observed during January – February and the second maxima during July – August which could be attributed to the convective mixing due to winter cooling and high winds, respectively as has been observed by Babu *et al.* (2004), Shetye (1986), Rao and Mathew (1990), and Rao and Sivakumar (1998). Low MLDs were observed during March – May, and September – November for all the years for MLD_A, with a similar trend observed for MLD_W. However, MLD_W is underestimated compared to MLD_A during the summer monsoon (JJAS), pre-monsoon (MAM) and winter monsoon (DJF) seasons and overestimated during post-monsoon (ON). This is observed for all the months except December 02 when WLD_W overestimates MLD_A, and again in October 03 when WLD_W underestimates MLD_A. This study revealed that MLD_A values did vary significantly from MLD_W in WIO for most part of the analysis. However, the MLD variability patterns observed in both the estimates are similar.

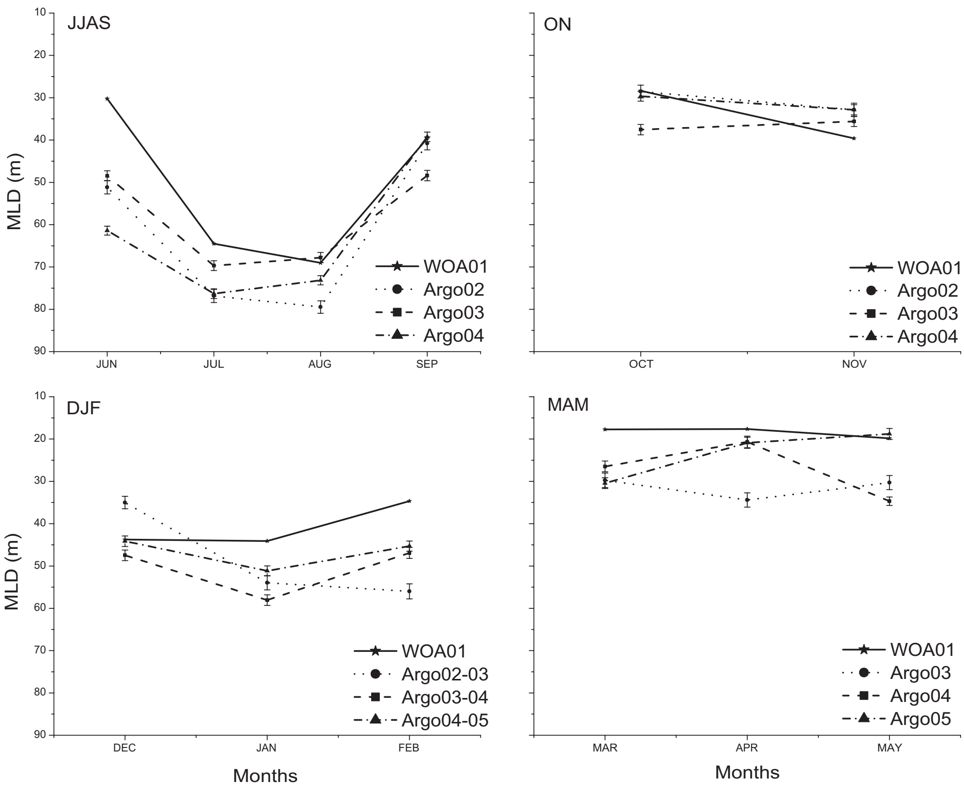

Figure 7. Comparison of monthly mean MLD estimates from WOA01 and Argo for the years 2002, 2003, 2004 and 2005.

The year to year variability of MLD in the central AS is summarized in Table 1. The maximum monthly average MLD obtained is presented in bold and minimum in bold italics for each of the years of study. The SD in the estimations are presented in braces. Maximum monthly mean MLD 0f 69 m was observed in August for MLD_W where as in case of Argo 2002, this was observed in August (~78 m), and for Argo 2003 (2004), maximum MLD of ~70 m (~74 m) was observed in July. Minimum monthly mean MLD was found in the month of April with values of 18 m (WOA01), ~30 m in March (Argo 2003), 30 m in April (Argo 2004), and ~20 m in May for Argo 2005.

4. Conclusions

MLD from Argo float T/S data was estimated and its variability was observed for three consecutive years starting from June 2002 to May 2005 for WIO. These MLD estimates were compared with MLD_W. The seasonal changes of MLD_A showed trends almost similar to those found in climatology throughout the study period. However, some inter-annual

Table 1. Monthly Average MLDs in central Arabian Sea from WOA01 (Jan–Dec), Argo 2002 (Jun–Dec), Argo 2003 (Jan–Dec), Argo 2004 (Jan–Dec) and Argo 2005 (Jan–May). The standard deviations for the MLD estimations are presented in braces.

MLD (m) (±SD) MONTH	WOA 01	ARGO 2002	ARGO 2003	ARGO 2004	ARGO 2005
JAN	44.1		54.6 (±1.6)	57.2 (±1.2)	50.1 (±1.1)
FEB	34.7		56.1 (±1.8)	46.9 (±1.3)	46.3 (±1.2)
MAR	17.7		30.4 (±1.7)	26.9 (±1.2)	30.4 (±1.3)
APR	17.6		34.6 (±1.7)	21.0 (±1.3)	21.4 (±1.3)
MAY	19.8		30.5 (±1.6)	35.6 (±1.0)	19.5 (±1.2)
JUN	30.2	50.9 (±1.5)	48.3 (±1.1)	60.3 (±1.0)	
JUL	64.5	75.7 (±1.6)	69.8 (±1.1)	74.4 (±1.1)	
AUG	69.0	77.5 (±1.5)	67.7 (±1.2)	72.0 (±1.0)	
SEP	39.6	41.2 (±1.5)	48.8 (±1.2)	38.1 (±1.1)	
OCT	28.34	28.8 (±1.5)	37.2 (±1.2)	29.8 (±1.2)	
NOV	39.6	33.2 (±1.6)	35.8 (±1.1)	32.6 (±1.1)	
DEC	43.7	35.5 (±1.5)	47.4 (±1.2)	43.8 (±1.2)	

variabilites did exist in MLD in terms of minimum and maximum values and their months of occurrence (as shown in Table 1). The R values between MLD_W and MLD_A are 0.60, 0.28, 0.67 and 0.40 for the months JJAS, ON, DJF and MAM, respectively. Further, seasonal averages of OLR and WS have been analyzed for the study period to qualitatively observe their impact on MLD variability. It is found that during the study period, MLD_W is underestimated as compared to MLD_A for almost all the months except November. This study demonstrates that Argo T/S profile data can be successfully used to study the spatial and seasonal variability of MLD and the Argo profiles were able to capture the effects of seasonal factors that affect MLD and mixed layer dynamics like wind, solar insolation and currents. With the availability of more number of Argo profiles in the future, the interannual variability studies of MLD and mixed layer heat budget can be successfully carried out with the possibility of incorporating these profiles data into ocean models. With availability of long term Argo data, a better climatology can also be constituted which will be a significant contribution for oceanographic studies.

Acknowledgments. The authors thank the Director, Indian National Centre for Ocean Information Services (INCOIS), for his encouragement. The valuable suggestions and comments from Dr. M. M. Ali, Head (OD), NRSA, Dr. D. Balasubrahamanyam, KORDI and Muni Krishna, RA, Meteorology and Oceanography Division, Andhra University are gratefully acknowledged. Argo data were collected and made freely available by the International Argo Project and the national programmes that contribute to it (http://www.argo.ucsd.edu, http://argo.jcommops.org). The authors wish to acknowledge use of the Ferret program, a product of NOAA's Pacific Marine Environmental Laboratory, for analysis and graphics in this paper. We thank the anonymous reviewers for their constructive suggestions.

REFERENCES

Ali, M. M. and R. Sharma. 1994. Estimation of mixed layer depth in the equatorial Indian Ocean using Geosat altimeter data. Mar. Geol., *17*, 63 – 72.

Argo Science Team. 2001. The Global Array of Profiling Floats, *in* Observing Oceans in the 21st Century, C. Z. Koblinsky and N. R. Smith, eds., Godae Proj. Off., Bur. Meteorol., Melbourne, Australia, 248 – 258.

Babu, K. N., R. Sharma, N. Agarwal, V. K. Agarwal and R. A. Weller. 2004. Study of mixed layer depth variations within the north Indian Ocean using a 1-D model. J. Geophys. Res., *109,* C08016, doi:10.1029/2003JC002024.

Brainerd, K. E. and M. C. Gregg. 1995. Surface mixed and mixed layer depths. Deep-Sea Res. I, *42*, 1521 – 1543.

Chen, D., L. M. Rothstein and A. J. Busalacchi. 1994. A hybrid vertical mixing scheme and its application to tropical ocean models. J. Phys. Oceanogr., *24*, 2156 – 2179.

Conkright, M. E., R. A. Locarnini, H. E. Garcia, T. D. O'Brien, T. P. Boyer, C. Stephens and J. I. Antonov. 2002. World Ocean Atlas 2001: Objective Analysis, Data Statistics, and Figures, [CD-ROM] Natl. Oceanogr. Data Cent., Silver Spring, MD.

de Boyer Montégut, C., G. Madec, A. S. Fischer, A. Lazar and D. Iudicone. 2004. Mixed layer depth over the global ocean: An examination of profile data and a profile-based climatology. J. Geophys. Res., *109,* C12003, doi: 10.1029/2004JC002378.

Düing, W. and A. Leetma. 1980. Arabian Sea cooling, a preliminary heat budget. J. Phys. Oceanogr., *10*, 307-312.

Findlater, J. 1969. A major low-level air current near the Indian Ocean during the northern summer. Q. J. R. Meteorol. Soc., *95*, 362 – 380.

Fischer, A. S. 1997. Arabian Sea mixed layer deepening during the monsoon: Observations and dynamics. M.S. thesis, MIT, Cambridge, MA.

——2000. The upper ocean response to the monsoon in the Arabian Sea. Ph.D. thesis, MIT/ WHOI Joint Program, Cambridge MA, 222 pp.

Godfrey, J. S. and A. Schiller. 1997. Tests of mixed-layer schemes and surface boundary conditions in an Ocean General Circulation Model, using the IMET flux data set. CSIRO Marine Lab. Report (231), Australia.

Kanegae, S. and M. Kubota. 2003. North Pacific mixed layer depth from Argo, poster in: First Argo Science Workshop, Nov. 12 – 14, 2003, Tokyo, Japan.

Kara, A. B., P. A. Rochford and H. E. Hurlburt. 2000. An optimal definition for ocean mixed layer depth. J. Geophys. Res., *105 (C7)*, 16,803 – 16,821.

Kessler, W. S. and J. P. McCreary. 1993. The annual wind-driven Rossby wave in subthermocline Equatorial Pacific. J. Phys. Oceanogr., *23,* 1192 – 1207.

Levitus, S. 1982. Climatological atlas of the world ocean, NOAA Prof. Paper, *13*, U.S. Govt. Print. Off., Washington, DC, 113 pp.

Longhurst, A. 1995. Seasonal cycles of pelagic production and consumption. Prog. Oceanogr., *36*, 77 – 167.

Lukas, R. and E. Lindstrom. 1991. The mixed layer of the western equatorial Pacific Ocean. J. Geophys. Res., *96,* 3343 – 3357.

McCreary, J. P. and P. K. Kundu. 1989. A numerical investigation of the sea surface temperature variability in the Arabian Sea. J. Geophys. Res., *94*, 16,097 – 16,114.

McCreary, J. P., P. K. Kundu and R. L. Molinari. 1993. A numerical investigation of dynamics, thermodynamics and mixed-layer processes in the Indian Ocean. Prog. Oceanogr., *31*, 181–244.

Millero, F. J., C. T. Chen, A. Bradshaw and K. Schleicher. 1980. A new high pressure equation of state for seawater. Deep-Sea Res., *27*, 255 – 264.

Montery, G. and S. Levitus. 1997. Seasonal variability of mixed layer depth of the world ocean. NOAA Atlas, NESDIS 14, Washington DC.
Morel, A. and J. M. Andre. 1991. Pigment distribution and primary production in the western Mediterranean as derived and modeled from coastal zone colour scanner observations. J. Geophys. Res., *96*, 685–698.
O'Brien, J. J. and H. E. Hurlburt. 1974. Equatorial jet in the Indian Ocean.Theory. Science, *184*, 1075 – 1077.
Ohno, Y., T. Kobayashi, N. Iwasaka and T. Suga. 2004. The mixed layer depth in the North Pacific as detected by the Argo floats. Geophys. Res. Lett., L11306, doi:10.1029/2004GL019576.
Prasad, T. G. 2004. A comparison of mixed-layer dynamics between the Arabian Sea and Bay of Bengal: One-dimensional model results. J. Geophys. Res., *109*, C03035, doi:10.1029/2003JC002000.
Prasad, T. G. and N. Bahulayan. 1996. Mixed layer depth and thermocline climatology of the Arabian Sea and western equatorial Indian Ocean. Indian J. Mar. Sci*., 25*, 189 – 194.
Price, J., R. Weller and R. Pinkel. 1986. Diurnal cycling: observations and models of upper ocean response to diurnal heating, cooling and wind mixing. J. Geophys. Res., *91,* 8411–8427.
Rao, R. R. and B. Mathew. 1990. A case study on the mixed layer variability in the south central Arabian Sea during the onset phase of MONEX-79. Deep-Sea Res., *37*, 227 – 243.
Rao, R. R. and R. Sivakumar. 1998. Observational variability of heat content in the upper layers of the tropical Indian Ocean from new global ocean temperature climatology. Deep-Sea Res. II, *45*, 67 – 89.
Ravichandran, M., P. N. Vinaychandran, S. Joseph and K. Radhakrishnan. 2004. Results from the first Argo float deployed by India*.* Curr. Sci., *86*, 651 – 659.
Schiller, A., J. S. Godfrey, P. McIntosh and G. Meyers. 1997. A Global Ocean General Circulation Model for Climate Variability Studies, CSIRO Marine Lab. Report (227), Australia.
Shetye, S. R. 1986. A model study of the seasonal cycle of the Arabian Sea surface temperature. J. Mar. Res., *44*, 521 – 542.
Suga, T. and K. Hanawa. 1990. The mixed layer climatology in the northwestern part of the North Pacific subtropical gyre and the formation area of Subtropical Mode Water. J. Mar. Res., *48,* 543 – 566.
Suga, T., K. Motoki, Y. Aoki and A. M. MacDonald. 2004. The North Pacific climatology of winter mixed layer and mode waters. J. Phys. Oceanogr., *34*, 3 – 22.
Thomson, R. E. and I. V. Fine. 2003. Estimating mixed layer depth from oceanic profile data. J. Atmos. Oceanic Technol*., 20*, 319 – 329.
Uehara, H., T. Suga, K. Hanawa and N. Shikama. 2003. A role of eddies in formation and transport of North Pacific Subtropical Mode Water. Geophys. Res. Lett., *30*, doi:10.1029/2003GL017542.
Wackernagel, H. 1998. Multivariate Geostatistics, 2nd ed., Springer-Verlag, NY, 291 pp.
Weller, R. A. and D. M. Farmer. 1992. Dynamics of the ocean mixed layer. Oceans, *35*, 46 – 55.
Weller R. A., A. S. Fischer, D. L. Rudnick, C. C. Eriksen, T.D. Dickey, J. Marra, C. Fox and R. Leben. 2002. Moored observations of upper-ocean response to the monsoons in the Arabian Sea during 1994–1995. Deep-Sea Res. II*, 49*, 2195 –2230.
Wong, A., R. Keeley, T. Carval and the Argo Data Management Team. 2004. Argo quality control manual, ver. 2.0b, Report, 23 pp.
Wyrtki, K. 1973. An equatorial jet in the Indian Ocean. Science, *181*, 262 – 264.

Received: *5 August, 2005*; revised: *3 February, 2006*.